2011 American Control Conference
on O'Farrell Street, San Francisco, CA, USA
June 29 - July 01, 2011

A Model Predictive Control Approach for a Parallel Hydraulic Hybrid Powertrain

Timothy O. Deppen, *Student Member*, *ASME*, Andrew G. Alleyne, *Senior Member*, *IEEE*, Kim Stelson, Jonathan Meyer

In this paper, a model predictive control (MPC) approach is presented for solving the energy management problem in a parallel hydraulic hybrid vehicle. The hydraulic hybrid vehicle uses a variable displacement pump/motor combination to transfer energy between the mechanical and hydraulic domains and a high pressure accumulator for energy storage. The proposed controller observes the gas and brake pedal positions to estimate the desired wheel torque. It regulates the engine throttle command, pump/motor displacement, and applied brake force to track this desired torque while optimizing the powertrain efficiency. Simulation studies were conducted to evaluate the effects of engine dwell time and accumulator capacity versus on the overall vehicle fuel economy.

I. Introduction

Hydraulic hybrid powertrain architectures present an opportunity to improve vehicle operating efficiency through the use of energy storage via a high pressure accumulator. This form of alternative energy storage has received growing attention due to its superior power density to electrical storage [1]-[4]. Furthermore, the accumulator can be safely charged and discharged repeatedly over the full range of storage capacity, allowing for greater flexibility in vehicle operation. To take advantage of the additional degrees of freedom present within the hydraulic hybrid powertrain, a supervisory control or energy management strategy (EMS) is needed to regulate the generation, storage, and distribution of energy within the powertrain.

Many approaches have been developed for defining such strategies. Most notably; rule based, stochastic dynamic programming (SDP), and model predictive control (MPC). Rule based EMS's use a set of rules or logic to control the powertrain [2], [5]. They are typically extrapolated from global optimization assessment performed using deterministic dynamic programming over an assumed drive cycle. Since the optimization is not causal, it is approximated with a causal logic. This logic can then be implemented in real time but it is suboptimal [3]. Due to the cycle-dependent nature of this derivation, the performance cannot be guaranteed under arbitrary driving. Stochastic dynamic programming uses probability maps in place of an assumed drive cycle to make an estimate of what the vehicle will be required to do in the future and optimizes using this estimate [3], [6]. The benefits of this approach over the rule based design are that the solution is not limited to a specific drive cycle and a causal control strategy is determined without further analysis of the results. However, this optimization procedure still includes some implicit assumption of the drive cycle.

Model predictive control is an attractive control method for passenger vehicle applications where the drive cycle is not known apriori, environmental variables can have a significant impact on driver behavior, and driver behavior can vary significantly between individuals. Unlike the rule based and SDP solutions, MPC uses no knowledge of the future drive cycle, or its statistical nature, to compute the control solution. Rather, a model of the system is used to predict how the powertrain will respond to a sequence of inputs. This enables one to transform a finite horizon objective function expressed in terms of the states and controls as just a function of the control. Therefore, the trajectory which minimizes the objective function is reduced to a sequence of control decisions. Since the MPC algorithm can be implemented without future knowledge, it has seen recent application in design of EMS's for hydraulic hybrids [7].

In this work, a model predictive controller will be presented for regulation of a parallel hydraulic hybrid vehicle (PHHV). The controller will regulate the engine throttle command, pump/motor displacement, and force applied to the brakes in order to ensure satisfaction of the operator's torque demand while imposing efficient operation of the overall powertrain. This work expands upon the previous study of MPC applied to the PHHV, [7], by incorporating engine and pump efficiency measures into the online optimization and introducing a driver within the loop.

The model of the PHHV will be described in section II. In section III, the model predictive control design will be explained. In section IV, simulation results will be given. Finally, section V provides conclusions and discussion points.

II. Powertrain Model

The parallel hydraulic hybrid powertrain uses a variable displacement pump/motor connected in parallel with the transmission to regulate the transfer of energy to/from the accumulator. This enables the storage of energy generated by the engine. This stored energy can be used to assist the engine or completely supply the operator's power demand. In addition, energy which is normally dissipated by mechanical brakes can

T. O. Deppen (tdeppen@illinois.edu) and A. G. Alleyne (alleyne@illinois.edu) are with the Mechanical Science and Engineering Department at the University of Illinois at Urbana-Champaign, Urbana, IL 61801 USA (phone: 217-244-9993; fax: 217-244-6534).

K. Stelson (kstelson@me.umn.edu) and J. Meyer (meyer994@umn.edu) are with the Mechanical Engineering Department at the University of Minnesota, Minneapolis, MN 55455 USA (phone: 612-625-6634; fax 616-626-7165).

978-1-4577-0079-8/11/$26.00 ©2011 AACC

be captured in the accumulator when decelerating. A schematic of the PHHV is presented in Fig. 1.

The parallel powertrain model presented here was designed for analysis of control performance and use in real time simulation. As such, it lacks the detail of high fidelity models but still captures the relevant dynamics of power transfer between the engine, wheels, and accumulator. It is an extension of a model, described in [7], which was developed using the Simscape/Simhydraulics toolboxes. In contrast with the model of [7], the pump/motor response in this work is captured in a look-up table and the Simscape and Simhydraulics toolboxes are no longer needed.

The proposed model represents a small passenger vehicle (similar in size to a Polaris Ranger) with a 2 gear transmission and a parallel hydraulic hybrid powertrain [8]. See appendix A for a list of the model parameters.

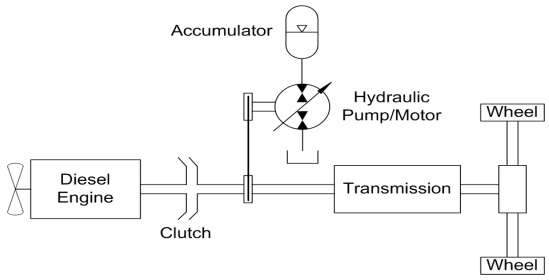

Fig. 1. Parallel Hydraulic Hybrid Vehicle

A. *Mechanical Elements*

The engine model employed in the PHHV model represents a Perkins 403C-11 Diesel engine. The dynamics of this engine were captured using the engine model presented in [9] with the torque output being scaled by 0.57. The efficiency characteristics of the engine were derived using the Willans line model and data provided by the manufacturer [10], see Fig. 2. Due to the limited data available when constructing the engine efficiency map, it was found that this mapping did not accurately characterize fuel consumption under idle conditions. Therefore, an experimentally validated fuel consumption rate of 0.08 kg/s is used when the engine is idling. The engine is connected to the powertrain via the clutch. This relationship is given by (1).

$$I_e\dot{\omega}_e = T_e - D_e\omega_e - T_c \tag{1}$$

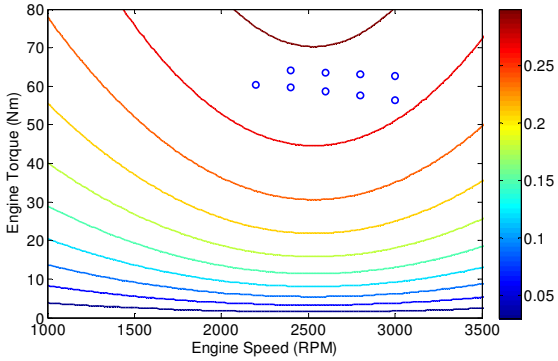

Fig. 2. Engine efficiency map with color bar indicating efficiency (ideal engine efficiency = 1). Blue circles indicated data points used to evaluate Willians line model.

Here I_e is the engine inertia, D_e is the engine damping coefficient, ω_e is the engine angular velocity, T_e is the engine torque, and T_c is the friction torque from the clutch.

The clutch friction torque, (2) and (3), is used to equilibrate the angular velocities of the clutch input and output shafts. The interaction between the flywheel and clutch plate is characterized by viscous and static friction.

$$T_c = 2/3 \cdot r_c \cdot F_{app} \cdot \mu \cdot sign(\omega_e - \omega_c) \tag{2}$$

$$\mu = |v_c \cdot (\omega_e - \omega_c)| + c_c \tag{3}$$

Here r_c is the radius of the clutch plate, F_{app} is the normal force applied to the clutch, ω_c is the angular velocity of the clutch output shaft, v_c is the viscous friction coefficient, and c_c is the coulomb friction coefficient.

The torque balance at the wheels is given by (4) through (7). Here R is the transmission ratio, T_H is the hydraulic load torque, T_b is the brake torque, I_t and D_t are the inertia and damping coefficients of the transmission input shaft, respectively, I_w and D_w are lumped inertial and damping coefficients of the wheel and transmission output shaft, respectively, and ω is the angular velocity of the wheels. The vehicle load (mass and air drag) are contained within T_{Load}, see (11).

$$I_L \cdot \dot{\omega} = R \cdot T_c - R \cdot T_H - T_{Load} - T_b - D_L \cdot \omega \tag{4}$$

$$I_L = R \cdot I_t + I_w \tag{5}$$

$$D_L = R \cdot D_t + D_w \tag{6}$$

$$\omega = \omega_c / R \tag{7}$$

The transient behavior of the transmission is modeled as a first order system with unity gain and a time constant of 1 second. This time constant was chosen based on survey results of automated manual transmissions [11].

The brake torque is computed using a reduced version of the model posed by Gerdes and Hedrick [12]. Their model is approximated as a first order system whose time constant is consistent with that of the original model for a median applied force. Equation (8) defines the relationship between applied force (F_b) and pressure (P_b).

$$P_b(s) = \frac{12000}{0.015\,s + 1} F_b(s) \tag{8}$$

The pressure is then translated into braking torque via the friction model given by (9) and (10).

$$T_b = 2/3 \cdot A_{pad} \cdot P_b \cdot \mu \cdot sign(\omega) \tag{9}$$

$$\mu = |v_b \cdot \omega| + c_b \tag{10}$$

Here A_{pad} is the area of the brake pad, ω is the angular velocity of the wheels, v_b is the viscous friction coefficient, and c_b is the coulomb friction coefficient.

Finally, the load torque, (11), accounts for the effect of vehicle mass (m), longitudinal tire force (F_x), and air drag (drag coefficient: C_d, vehicle area: A_{veh}, air density: ρ_{air}). The equation of motion for the vehicle operating under these loads is given by (12).

$$T_{Load} = r \cdot F_x \tag{11}$$

$$\dot{v}_{veh} = \left[F_x - 0.5 \cdot \rho_{air} \cdot C_d \cdot A_{veh} \cdot v_{veh}^2 \right] / m \quad (12)$$

Here r is the wheel radius and v_{veh} is the vehicle linear velocity.

The longitudinal tire force is computed using a simple linear tire model given in (13). The linear tire model assumes good surfaces and low slip, thereby enabling the use of a linear relationship between the slip ratio and tractive force. To compensate for small wheel velocities, a lower bound on the denominator is applied ($v_{\min}$).

$$F_x = \begin{cases} K\left(1 - v_{veh} / (r \cdot \omega)\right) & \text{For } r \cdot \omega \geq v_{\min} \\ K\left((r \cdot \omega - v_{veh}) / v_{\min}\right) & \text{For } r \cdot \omega < v_{\min} \end{cases} \quad (13)$$

Here K is the slip coefficient, r is the wheel radius, ω is the angular velocity of the wheels.

B. Hydraulic Elements

There are three elements to the hydraulic circuit: the variable displacement pump/motor, the 2 way directional valve, and the high pressure accumulator. The variable displacement pump/motor is modeled using a map of data points for a 28 cc/rev Sauer-Danfoss variable displacement axial piston pump. This map reads in the angular velocity of the pump drive shaft (ω_p), pressure (P), and displacement (x [0,1]) and outputs the required torque (T_H) and volumetric flow (Q). Equations (14) and (15) capture this relationship.

$$T_H = Map_T(\omega_p, P, x) \quad (14)$$

$$Q = Map_F(\omega_p, P, x) \quad (15)$$

When operating as a hydraulic motor (x [-1,0]), a separate set of data points are used but the inputs are the same.

The 2 way directional valve is used to connect the high pressure accumulator with the hydraulic circuit. This valve is used strictly in an on/off fashion. As such, its dynamics have been ignored at present. The logic for when the valve is open and closed is presented in section III.

The accumulator model represents a gas charged accumulator in which high pressure fluid is used to compress gas which is separated from the fluid via a flexible membrane. When the pressure at the inlet of the accumulator falls below the gas pressure, fluid is forced out of the accumulator as the gas expands. Equation (16) captures this relationship assuming ideal gas behavior. To prevent a discontinuity in accumulator pressure, a linear approximation is made for small oil volumes.

$$P = \begin{cases} P_{pr} \cdot (V_{\max} \cdot V_{acc}) / (V_{nom}(V_{\max} - V_{nom})) & \text{for } V_{acc} \leq V_{nom} \\ P_{pr} \cdot V_{\max} / (V_{\max} - V_{acc}) & \text{for } V_{acc} > V_{nom} \end{cases} \quad (16)$$

Here V_{acc} is the fluid volume within the accumulator, V_{max} is the maximum accumulator capacity, P_{pr} is the gas precharge pressure, P is accumulator pressure, and V_{nom} is the small volume at which the linearized approximation ends.

C. Driver Model

The driver model consists of a pair of PI controllers, one for each pedal, with integral anti-windup. A relay, given by (17), is used to switch between applying the gas and brakes.

$$Mode(t) = \begin{cases} 1 & \text{For } e > 0.5 \\ -1 & \text{For } e < -2 \\ Mode(t-1) & \text{For } -2 \leq e \leq 0.5 \end{cases} \quad (17)$$

Here e is the difference between desired and actual vehicle velocity. When *Mode* is equal to one the gas is applied, when *Mode* is equal to minus one, the brakes are applied.

III. Control Design

The goal of the proposed controller is track the operator's desired torque at the wheels while imposing efficient operation of the engine and variable displacement pump\motor. To accomplish this regulation, a discrete model predictive control was designed. Discrete MPC is a feedback controller which utilizes a discrete model of the system to predict how the system will respond to a sequence of inputs over a finite horizon. In this way, the value of an objective function at each time step within the prediction horizon is a function of the current and previous control decisions within the prediction horizon. Thus, minimization of an objective function is reduced to selecting the appropriate sequence of inputs. The first element of the input sequence is applied to the system, and then the process is repeated at the next time step. For additional details, the reader is referred to [13]. This type of control has seen recent application to both the electric and hydraulic hybrid vehicles [7], [14].

The controller is composed of 3 main parts; pedal interpretation, prediction model, and optimization routine with supervisor. See Fig. 3 for a schematic of the controller. Measurements of the wheel angular velocity, accumulator state of charge (pressure), transmission gear ratio, displacement, and desired engine torque from the controller are made in order to perform the linearization and optimization.

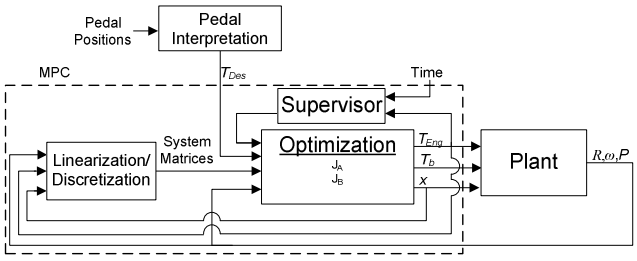

Fig. 3. Schematic of MPC

A. Pedal Interpretation

The operator communicates his or her desired performance to the EMS via the pedal positions, which are interpreted as a desired torque. The gas pedal position is translated into a desired wheel torque via a map which relates the pedal position and engine speed to engine torque. The resulting engine torque is multiplied by the transmission gear ratio. The mapping was derived by evaluating the torque output of the engine model for fixed engine speeds and throttle commands. The brake pedal position is translated to desired wheel torque via multiplication of the constants from the brake model given in section II, see (8) through (10), minus the coulomb friction term. The pedal position, θ_b (deg), is translated into force applied to the brakes via a constant.

B. Prediction Model

The prediction model used within the MPC contains simplified powertrain dynamics to facilitate rapid on-line solutions to the optimization problem. These dynamics are given by (18) through (25). This prediction model simplifies the previous vehicle model as follows: it ignores the engine and brake dynamics; the vehicle loads are reduced to a single inertia and damping term; the pump/motor dynamics are approximated by bilinear expressions based on the current operating conditions; and the accumulator dynamics are approximated as a collection of linear relationships.

$$I\dot{\omega} = R \cdot T_{eng} - R \cdot T_H - T_b - D\omega \tag{18}$$

$$\dot{P} = M \cdot Q \tag{19}$$

$$T_H = A_T \cdot x \cdot P + B_T \tag{20}$$

$$Q = A_Q \cdot x \cdot R \cdot \omega + B_Q \tag{21}$$

$$A_Q = \frac{\left[Map_F(\omega_{\max}, P_o, 1) - Map_F(\omega_{\max}, P_o, -1)\right] - \left[Map_F(\omega_{\min}, P_o, 1) - Map_F(\omega_{\min}, P_o, -1)\right]}{2(\omega_{\max} - \omega_{\min})} \tag{22}$$

$$B_Q = Map_F(\omega_o, P_o, x_o) - A_Q \omega_o x_o \tag{23}$$

$$A_T = \frac{\left[Map_T(\omega_o, P_{\max}, 1) - Map_T(\omega_o, P_{\max}, -1)\right] - \left[Map_T(\omega_o, P_{\min}, 1) - Map_T(\omega_o, P_{\min}, -1)\right]}{2(P_{\max} - P_{\min})} \tag{24}$$

$$B_T = Map_T(\omega_o, P_o, x_o) - A_T P_o x_o \tag{25}$$

Here I is the lumped vehicle inertia, ω is the angular velocity of the wheels, R is the transmission ratio, T_{eng} is the engine torque, T_H is the hydraulic load torque, T_b is the brake torque, D is the lumped damping coefficient, P is the accumulator pressure, M is defined by the linearized accumulator dynamics, Q is the flow rate into the accumulator, x is the displacement command (x [-1,1]), and subscript o denotes operating point. See appendix A for values used to define the prediction model.

To reduce the computational complexity of the optimization, the prediction model is linearized using a first order Taylor series approximation, (26) through (29). Here ω_o, x_o, and P_o denote the operating point with respect to angular velocity, displacement, and pressure. Note that this model is not fixed, the transmission ratio, M, and the pump/motor coefficients, see (22) through (25), are also dependent on the current operating condition. The linearized system is then discretized using the zero order hold method.

$$\begin{bmatrix} I & 0 \\ 0 & 1 \end{bmatrix} \begin{Bmatrix} \dot{\omega} \\ \dot{P} \end{Bmatrix} = \begin{bmatrix} -D & -R \cdot A_T \cdot x_o \\ M \cdot A_Q \cdot R \cdot x_o & 0 \end{bmatrix} \begin{Bmatrix} \omega \\ P \end{Bmatrix} + \begin{bmatrix} R & -1 & -R \cdot A_T \cdot P_o & 1 & 0 \\ 0 & 0 & M \cdot A_Q \cdot R \cdot \omega_o & 0 & 1 \end{bmatrix} \cdot U \tag{26}$$

$$U^T = \begin{Bmatrix} T_{eng} & T_b & x & L_1 & L_2 \end{Bmatrix} \tag{27}$$

$$L_1 = R \cdot A_T \cdot P_o \cdot x_o - R \cdot B_T \tag{28}$$

$$L_2 = -M \cdot A_Q \cdot R \cdot \omega_o \cdot x_o + B_Q \tag{29}$$

The prediction model showed good agreement with the model described in section II. Fig. 4 shows a comparison of the two models, when the prediction model is updated every 5 seconds. For this simulation, the engine torque was stepped from 0 to 40 Nm at time 0 and the displacement was held constant at 0.1. This represents a moderate acceleration while slowly charging the accumulator.

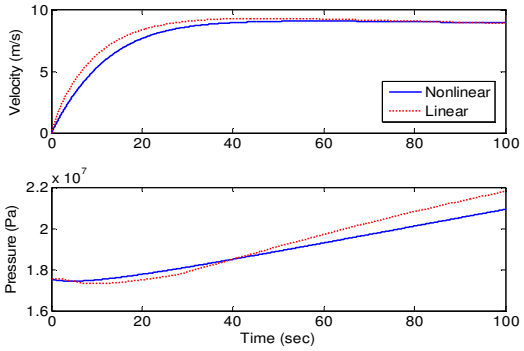

Fig. 4. Comparison the simulated vehicle velocity and accumulator pressure between the model from section II and prediction model.

C. Objective Functions

Two objective functions are utilized within the MPC; one for when the desired torque is positive and one for when the desired torque is negative. They are denoted by J_A and J_B respectively and are defined by (30) through (33). The integral of the cumulative deviation from the desired values over the prediction horizon is used when evaluating the cost of a policy. This more heavily penalizes deviation from the desired values at the beginning of the prediction horizon, thereby improving tracking performance. The primary goal of J_A and J_B is to track the desired wheel torque as interpreted by the pedal positions.

The definition of the secondary objective used within J_A and J_B was motivated by an analysis of the component efficiencies. When the wheel torque demand is positive, power can be supplied with or without the engine. When engine power is used, to maximize its efficiency for a prescribed velocity, its torque output should also be maximized, see Fig. Fig. **2**. Similarly, to maximize pump/motor efficiency, its displacement should be maximized. These two objectives are complimentary since maximizing engine torque maximizes excess power generation thereby forcing the pump to operate at higher displacement. When engine power is not needed, the system no longer has excess degrees of freedom and the pump/motor displacement is constrained by the operator's demand. Therefore, when the desired wheel torque is positive the efficiency objective of the control will focus solely on tracking a desired engine torque.

When the desired wheel torque is negative, one wishes to maximize the captured energy, therefore the secondary objective is formatted as tracking the maximum pump/motor displacement $x_{Des} = 1$.

$$J_A = \sum_{j=0}^{n-1} \sum_{i=0}^{j} \overbrace{\lambda_1 \left(\frac{T_A(i) - T_{Des}}{T_{Des,\max}} \right)^2}^{\text{Primary}} + \overbrace{\lambda_2 \left(\frac{T_{eng}(i) - T_{eng,Des}}{T_{eng,\max}} \right)^2}^{\text{Secondary}} \tag{30}$$

$$J_B = \sum_{j=0}^{n-1} \sum_{i=0}^{j} \underbrace{\lambda_1 \left(\frac{T_B(i) - T_{Des}}{T_{Des,\max}} \right)^2}_{\text{Primary}} + \underbrace{\lambda_2 \left(x(i) - x_{Des} \right)^2}_{\text{Secondary}} \tag{31}$$

$$T_A(i) = R \cdot T_{eng}(i) - R\left(A_T \left(x_o \cdot P(i) + P_o \cdot x(i) - x_o P_o \right) + B_T \right) \tag{32}$$

$$T_B(i) = T_b(i) + R\left(A_T\left(x_o \cdot P(i) + P_o \cdot x(i) - x_o P_o\right) + B_T\right) \quad (33)$$

Here n is the number of steps in the prediction horizon, subscript *Des* denotes the desired value, and subscript *max* denotes maximum value. The desired torque tracking term and the engine torque term are divided by their respective maximum values to normalize the resulting cost. The final objective functions are quadratic and were solved using the "quadprog" command from the Matlab optimization toolbox.

A supervisory logic is applied to prevent high frequency cycling of the engine on and off. If the J_A objective function is used, the default desired engine torque is $T_{eng,Des}$ = 0 Nm. This penalizes engine use forcing the system to run on stored energy. The supervisor monitors the commanded engine torque for when it has exceeded a threshold, $T_{threshold}$

$$T_{eng} \geq T_{threshold} \quad (34)$$

Once this condition has occurred, the desired engine torque changes to full throttle, $T_{eng,Des}$ = 70 Nm. This value is maintained until T_{dwell} time has passed. After the dwell time has passed, the logic checks if the desired torque is less than a threshold. By defining this threshold as done in (35), one can use it to ensure that there is sufficient charge in the accumulator to sustain the desired wheel torque.

$$T_{Des} \leq R \cdot X_{\max} \cdot k \cdot P \quad (35)$$

Here an ideal pump model has been assumed, T_{Des} is the desired wheel torque, R is the gear ratio, X_{max} is the maximum pump/motor displacement, P is the accumulator pressure, and k is a constant ranging between 0 and 1 which can be used to tune how aggressively the supervisor seeks to declutch the engine and run on stored energy.

Finally, at low speeds (ω < 13 rad/sec) the leakage losses of the pump/motor dominate. Therefore, under these conditions the two way valve joining the accumulator to the hydraulic circuit is closed and the displacement is forced to be zero. Thus only the primary term of J_A and J_B is considered.

D. Constraints

For control of the PHHV, constraints are needed for the allowable accumulator pressure. A lower bound is needed to prevent the controller from attempting to remove oil from an empty accumulator and an upper bound is needed to prevent the system from exceeding the maximum allowable pressure of the hydraulic components. The upper and lower bound were set to 12.5 MPa (10% maximum allowable oil volume) and 35 MPa.

IV. Results

Using the control strategy described in section III, a simulation study was conducted to evaluate the relationship between the dwell time, accumulator capacity, and powertrain performance. For this simulation study, an update rate of 2 Hz was used and the prediction horizon was 5 seconds. This prediction horizon has been used successfully in other hybrid vehicle research [7], [14]. The update rate was chosen to be as small as possible, while ensuring sufficient time for the MPC to solve between updates. Using a computer with a 2.6 GHz processor and 8 GB RAM, the combined average linearization and optimization computation time was approximately 0.05 seconds. For the supervisor the engine threshold, (34), was set to 10 Nm and k from (35) was set to 0.5. In each simulation, the driver model used the EPA Urban Dynamometer Driving Schedule (UDDS) [15]. However, since this small passenger vehicle is not capable of traversing this profile, the velocities were scaled by a factor 0.6.

The results of the simulation study shown in Fig. 5 demonstrate that there is a clear tradeoff between dwell time and fuel economy. For dwell times less than 5 seconds both the engine and pump/motor lose efficiency during transients associated with the many charging events. As the dwell times increases, up to 20 seconds, the average efficiency when the engine was clutched improved for all accumulator sizes since there are fewer transients. However, for dwell times in excess of 20 seconds, the average engine efficiency when clutched decreases due to accumulator saturation which prevents efficient engine operation. Naturally, this effect is less pronounced for the larger accumulator. In addition, as the dwell time increases there is a significant reduction in average displacement when motoring; at T_{dwell} = 30 sec the average motor displacement was 25% less than at T_{dwell} = 7 sec for the 10 gal. accumulator. This results in a net loss in efficiency and consequently a decrease in fuel economy. The maximum fuel economy was observed for dwell times between 5 and 15 seconds because there was balance between efficiency loss due to transients and low motoring displacement. Similar tradeoffs have been observed in other hydraulic hybrid studies [3]. For larger accumulators the dwell time range over which one achieves this balance is slightly larger because there is a smaller pressure increase per unit flow.

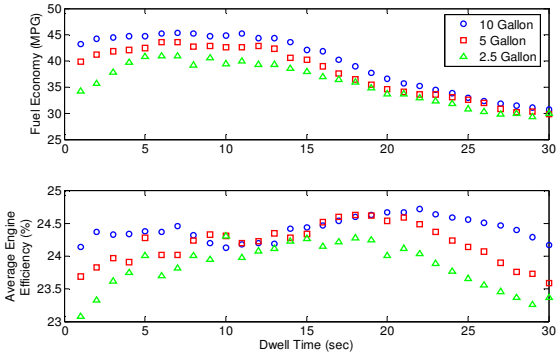

Fig. 5. Fuel economy and average engine efficiency when clutched for varying dwell time and accumulator capacity

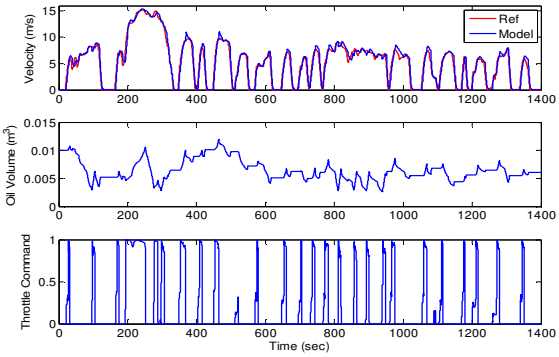

Fig. 6. Powertrain response for 10 gallon accumulator and T_{dwell} = 7 sec

Fig. 6 shows the powertrain response for the best fuel economy trial from the simulation study (10 gallon accumulator, T_{dwell} = 7 sec). From these results one can see that the MPC was able to track the operators torque demand while using the engine in an on/off fashion. Furthermore, only a small portion of the accumulator was used (45% of max allowable volume at peak charge) enabling the pump/motor to operate at larger displacement during motoring operation.

To benchmark these simulation results, a non-hybrid vehicle was simulated using the same parameters and it achieved an average engine efficiency when clutched of 17.9% and a fuel economy of 30.5 MPG. For the best case fuel economy scenario from Fig. 5, the hybrid powertrain achieved 24.5% average clutched engine efficiency (an improvement of 35%) and a fuel economy of 45.3 MPG (an improvement of 48.5 %).

V. Conclusion

A model predictive controller was successfully able to track the desired wheel torque, while utilizing the energy storage capabilities to improve fuel economy and a dwell time constraint to prevent high frequency cycling of the engine. However, it was observed that the dwell time constraint can have a significant impact on fuel economy. When sizing the accumulator for the parallel powertrain, one must consider the allowable engine cycling frequency. If a large dwell time is required to prevent wear on the engine, then a suitably large accumulator should be used to prevent accumulator saturation and to enable more efficient motoring of the pump/motor.

Future work will focus on validating these results on an experimental system [8], and applying MPC to more complex hybrid powertrain architectures; the series and power split.

Appendix A

Below is a list of the parameter values used in the study.

Table I
Powertrain Parameters

I_e	0.145 kgm^2	c_b	0.001
D_e	0.106 Nm/(rad/s)	v_b	0.2 s/rad
r_c	0.1 m	r	0.31 m
v_c	0.2 s/rad	C_d	0.4
c_c	0.001	A_{veh}	2 m^2
R	7.5:1 (1st gear) 2.9:1 (2nd gear)	K	80000 N
I_t	0.065 kgm^2	$v_{\min}$	0.1 m/s
I_w	1.4 kgm^2	P_{pr}	11.7 MPa
D_t	0.001 Nm/(rad/s)	X_{max}	4.5x10^{-6} m^3/rad
D_w	1.0 Nm/(rad/s)	V_{max}	0.04 m^3
A_{pad}	0.01 m^2	V_{nom}	0.001 m^3
m	750 kg + (64.9: 2.5 gal, 92.8: 5 gal, 155.6: 10 gal)		

Table II
Prediction Model Parameters

I	81 kgm^2 (Clutch Locked) 80 kgm^2 (Clutch Unlocked)	R	7.5:1 (first gear) 2.9:1 (second gear)
D	7.5 Nm/(rad/s)	$\omega_{\min}$	0 rad/s
P_{min}	3 MPa	$\omega_{\max}$	500 rad/s
$P_{\max}$	35 MPa		

Table III
Linearized Accumulator Parameters: 10 gallon

Oil Volume Range (m^3)	M
0-0.001	1.21x10^{10}
0.001-0.005	3.4x10^8
0.005-0.01	4.5x10^8
0.01-0.015	6.2x10^8
0.015-0.0175	8.3x10^8
0.0175-0.02	10.4x10^8
0.02-0.0225	13.4x10^8
0.0225-0.025	17.8x10^8
0.025-0.0275	25.0x10^8
0.0275-0.029	34.0x10^8

Acknowledgment

This work was performed within the Engineering Research Center for Compact and Efficient Fluid Power (CCEFP), supported by the National Science Foundation under Grant No. EEC-0540834.

References

[1] Z. Filipi, Y. J. Kim, "Hydraulic Hybrid Propulsion for Heavy Vehicles: Combining the Simulation and Engine-In-the-Loop Techniques to Maximize the Fuel Economy and Emission Benefits," *Oil & Gas Science and Technology*, 65(1), pp. 155–178, 2010.

[2] B. Wu, C. C. Lin, Z. Filipi, H. Peng, D. Assanis, "Optimal power management for a hydraulic hybrid delivery truck," *Vehicle System Dynamics*, 42(1-2), pp. 23–40, 2004.

[3] R. Johri, Z. Filipi, "Low-cost pathway to ultra efficient city car: Series hydraulic hybrid system with optimized supervisory control," *SAE International Journal of Engines*, 2(2), pp. 505–520, 2010.

[4] K. A. Stelson, J. J. Meyer, "Optimization of a Passenger Hydraulic Hybrid Vehicle to Improve Fuel Economy". *7th JFPS International Symposium on fluid Power*, 2008.

[5] Z. Filipi, L. Louca, B. Daran, C. C. Lin, U. Yildir, B. Wu, M. Kokkolaras, D. Assanis, H. Peng, P. Papalambros, J. Stein, D. Szkubiel, R. Chapp, "Combined optimisation of design and power management of the hydraulic hybrid propulsion system for the 6 x 6 medium truck," *International Journal of Heavy Vehicle Systems*, 11(3-4), pp. 372–402, 2004.

[6] J. J. Meyer, K. A. Stelson, A. G. Alleyne, T. O. Deppen, "Power Management Strategy for a Parallel Hydraulic Hybrid Passenger Vehicle Using Stochastic Dynamic Programming," *Proc. of 7th International Fluid Power Conference*, 2010.

[7] T. O. Deppen, A.G. Alleyne, K. A. Stelson, J. J. Meyer, "Predictive Energy Management for Parallel Hydraulic Hybrid Passenger Vehicle," *Proc. of the ASME Dynamic Systems and Control Conference*, DSCC 2010.

[8] K. Kopplin, "Finding the right tool for the job," *Diesel Progress North American Edition*, pp. 40-41, 2010

[9] D. Cho, and K. J. Hedrick, "Automotive powertrain modeling for control," *Transactions of the ASME Journal of Dynamic Systems Measurement and Control*, 111(4), pp. 568–576, 1989.

[10] J. B. Heywood, *Internal Combustion Engine Fundamentals*, McGraw-Hill, New York, 1988.

[11] J.C. Wheals, C. Crewe, M. Ramsbottom, S. Rook, M. Westby, "Automated Manual Transmissions – a European Survey and Proposed Quality Shift Metrics, SAE Paper 2002-01-0929, 2002.

[12] J. C. Gerdes, and K. J. Hedrick, "Brake system modeling for simulation and control," *Transactions of the ASME Journal of Dynamic Systems Measurement and Control*, 121(3), pp. 496–503, 1999.

[13] J. M. Maciejowski, *Predictive Control with Constraints*, Prentice Hall, 2002.

[14] H. A. Borhan, A. Vahidi, A. M. Phillips, M. L. Kuang, I. V. Kolmanovsky, "Predictive energy management of a power-split electric hybrid vehicle," *Proc. of the American Control Conference*, 2009.

[15] http://www.epa.gov/nvfel/testing/dynamometer.htm#vehcycles